Modeling Financial Losses Resulting from Tornadoes in European Countries

JÜRGEN GRIESER AND FRANCESCA TERENZI

Risk Management Solutions, London, United Kingdom

(Manuscript received 19 May 2015, in final form 29 March 2016)

ABSTRACT

Tornadoes are a notorious, common threat to human life and property in the United States. Although less common, violent tornadoes are also reported in Europe. The authors aim for an estimation of the average annual loss ratio of European buildings due to tornadoes. An aggregated loss model is used that takes as input the tornado intensity distribution over the Fujita scale (F scale), the distribution of tornado footprint sizes per F class, the vulnerability of European buildings, and the average occurrence rate of tornadoes. Information about these variables is taken from the European Severe Weather Database and, where needed, from the U.S. Storm Prediction Center tornado database, which contains about 16 times more records. However, both databases are biased. Weak tornadoes are underrepresented. Therefore a bias-corrected tornado intensity distribution is used, with its uncertainty taken from the literature. Individual tornadoes are modeled as moving Rankine vortices creating elliptic footprints with correlated length and width. This allows for the estimation of the area fraction of a tornado footprint with lower wind speeds than the maximum wind speed, which is generally used to attribute an intensity. This approach is applied to define effective vulnerability functions of European buildings. A major result is that an expected 90% of the tornadoes contribute only about 1% to the average loss, while the rare F4 tornadoes contribute more than 40% of losses. Given that most national tornado databases in Europe contain tornado records for recent years only and few (if any) violent tornadoes, observed losses can lead to a remarkable underestimation of tornado risk in Europe.

1. Introduction

While the United States experiences approximately 100 violent tornadoes per decade, violent tornadoes are seen as extremely rare events in Europe. However, there is historical evidence that violent tornadoes and tornado outbreaks do actually happen in Europe. Some examples of those tornadoes are provided in Table 1.

The number of tornadoes recorded in the European Severe Weather Database (ESWD) has steeply increased during the last decade (Groenemeijer and Kühne 2014) due to an increase in both general interest and awareness of this weather phenomenon. This is possible thanks to improved methods to obtain, transfer, and collect information, such as digital photography, the Internet, and the establishment of databases such as the ESWD. However, nearly all of the tornadoes observed in Europe today are weak tornadoes, and this can pave the way to the misleading assumption that tornadoes in this continent are weak in general, with few exceptions like the outbreak on 3 and 4 August 2008 with 13 tornadoes (including one F4 tornado damaging 1000 buildings and causing three fatalities in Hautmont, France) and the F4 tornado in Veneto (Italy) on 8 July 2015 [for details, see ESSL (2015)].

According to Table 1, devastating tornadoes are rare events, but the case of an urban center being hit again by a violent tornado, leading to severe damage to properties and loss of lives, might merely be a matter of time. The increase in population and urbanization across Europe may also lead to an increase in the risk of tornado strikes in European urban areas. This gives rise to several questions, including the following:

1) What can we learn about the frequency of occurrence of violent tornadoes from short-term observation records?
2) How likely is an urban center to be hit by a violent tornado in Europe?
3) What is the average annual loss (AAL) ratio (AALR) due to tornadoes?
4) What influence do the violent but very rare tornadoes have on the AALR?

Corresponding author address: Risk Management Solutions Ltd., Peninsular House, 30 Monument Street, London EC3R 8NB, United Kingdom.
E-mail: juergen.grieser@rms.com

DOI: 10.1175/WCAS-D-15-0036.1

© 2016 American Meteorological Society

Downloaded from http://journals.ametsoc.org/doi/pdf/10.1175/WCAS-D-15-0036.1 by guest on 22 October 2020

TABLE 1. Some major tornado events in Europe, as reported by Grazulis (2001) (source 1), the European Severe Weather Database (ESWD; source 2), The Tornado and Storm Research Organization (TORRO; source 3), Wikipedia (source 4), and the European Severe Storms Laboratory (ESSL; source 5).

Date	Source	Location	Details
17 Oct 1091	1	London (United Kingdom)	600 wooden houses destroyed, possibly F4 tornado
23 Sep 1551 (1556)	3	Malta	Waterspout sank ships and killed at least 600 people, possibly the deadliest incidence
29 Jun 1764	2	Woldegk (Germany)	F5 tornado
23 Apr 1800	2	Hainichen (Germany)	F5 tornado
19 Aug 1845 (1849)	1	Monville (France)	Destroyed four-story stone building, killed all inside (70–200), possibly the strongest incidence
Dec 1851	4	Sicily (Italy)	Pair of tornadoes killed at least 500 people, among the deadliest incidences
10 Jul 1916	2	Vienna (Austria)	Severely damaged or destroyed 150 buildings, F3 tornado, Austrian deadliest/strongest incidence
24–25 Jun 1967	1	Belgium, Netherlands, France, Germany	Western Europe tornado outbreak, at least one F5, more than 15 fatalities
11 Sep 1970	1	Venice (Italy)	Venice and Padua, Italy tornado outbreak, up to F4, 36 fatalities
6 Jun 1984	1	Russia	300 km north of Moscow, killed about 400 people, outbreak with at least one F5
8 Jul 2015	5	Venice (Italy)	Outbreak with at least one F4, about 500 buildings badly damaged or destroyed in the Riviera del Brenta; seventeenth-century Villa Fini razed to the ground

5) Is it possible to address the above questions even though data and information are limited and might be biased?

In this paper we deal with these questions starting with a short overview of how the AAL of natural disasters is estimated with detailed loss models by the (re)insurance industry (section 2). In the same section we also derive an approximated equation for the aggregated AALR due to tornadoes at country-level resolution. This has the advantage of allowing loss estimates when only limited knowledge is available, as explained therein. Section 3 deals with a model for tornado hazards and aims to estimate tornado intensity, rate, and footprint size. We not only provide best estimates of these key variables but also estimate their uncertainty based on available observations. In section 4 an effective vulnerability function is introduced taking into account that tornado intensity is a measure of maximum wind speed within a tornado swath, whereas most of the footprint area might be affected by lower wind speeds. By propagating these best estimates and their uncertainties through the simplified loss model we provide best estimates for the AALR given today's observations and their uncertainties. Finally, the strategy is applied to data from several European countries and results are provided in section 5. Section 6 contains a final discussion.

2. Modeling tornado losses

a. A detailed view

Detailed loss models are based on synthetic event sets usually covering at least thousands of modeled years. They represent an ensemble of possible different realizations of what might occur next year. Each event i is characterized by a rate of occurrence R_i, a hazard extent or footprint area A_i, and a hazard severity $H_{n,i}$ describing the hazard intensity of event i at location n within its footprint. All property exposure that lies within the footprint area of an event gets hit by it. The damage that an event causes to a specific property at a given location, or an exposed subject at risk, depends on its structural characteristics represented by the specific vulnerability V_n of this subject. The loss due to each individual event can be calculated if all the exposure hit by the event, the local intensity of the event at the location of the exposure, and the specific vulnerability of the exposure are all known.

One of the central variables in risk modeling is the AAL. It is defined as

$$\mathrm{AAL} = \sum_{n=1}^{N} \sum_{i=1}^{I} E_n R_{n,i} V_n(H_{n,i}), \tag{1}$$

where E_n is the monetary value of the subject at risk at the location n, and $R_{n,i}$ is the rate at which the exposure is hit by the event i. The term V_n is the vulnerability function measuring the damage ratio that a given hazard can inflict upon E_n; V_n translates hazard intensity into a loss ratio.

Detailed loss models provide solutions of Eq. (1). While applying this detailed strategy allows answering a variety of questions, a solution is only possible when detailed information for local frequency, hazard intensity, exposure distribution, and vulnerability are available. Given our limited knowledge of tornado occurrence

Downloaded from http://journals.ametsoc.org/doi/pdf/10.1175/WCAS-D-15-0036.1 by guest on 22 October 2020

rate and intensity in Europe, we now turn to simplify Eq. (1).

b. The aggregated view

The intensity of tornadoes is usually registered in classes related to the degree of damage from wind speed intervals on manmade structures. The most-used classifications are the T classification from the Tornado and Storm Research Organisation (TORRO; http://www.torro.org.uk; Meaden 1976), the Fujita (F) scale (Fujita and Pearson 1973), or the Enhanced Fujita (EF) scale (McDonald et al. 2006). For details on the various classifications and their comparison, see Dotzek et al. (2003) and Doswell et al. (2009). In here we use the F scale and, instead of considering individual tornado intensities, we attribute one of the six F classes (0 to 5) to each tornado. This simplifies Eq. (1) considerably to

$$\mathrm{AAL} = \sum_{n=1}^{N} \sum_{\mathrm{F}=0}^{5} E_n R_{n,\mathrm{F}} V_n(H_{n\mathrm{F}}). \tag{2}$$

Furthermore, instead of looking at each individual building separately we aggregate the value of all buildings in an area, say a country, and use an average vulnerability function for buildings in this area. This leads to

$$\mathrm{AAL}_A = E_A \sum_{\mathrm{F}=0}^{5} R_{A,\mathrm{F}} V_A(H_\mathrm{F}), \tag{3}$$

where the index A indicates area-specific variables. In doing so, we assume that the spatial distributions of exposure and tornadoes within a country are statistically independent variables.

Finally, as mentioned in section 1, the aim of this study is to estimate AALR due to tornadoes for various countries in Europe. Hence we are only interested in the loss ratio defined as $\mathrm{AALR} = \mathrm{AAL}/E$. We can thus dispense with the exposure and get an expression for the AALR in this simplified aggregate loss model as

$$\mathrm{AALR}_A = \frac{\mathrm{AAL}_A}{E_A} = \sum_{\mathrm{F}=0}^{5} R_{A,\mathrm{F}} V_A(H_\mathrm{F}). \tag{4}$$

To obtain country-specific AALR we need to estimate country-specific tornado occurrence rates $R_{C,\mathrm{F}}$ and vulnerability functions V_C as well as tornado hazard intensities H_F. In the following two sections we describe how we model these three variables.

3. Modeling tornado hazard

The key variable for modeling tornado loss is the tornado intensity distribution. It allows for the deduction of intensity specific occurrence rates per area from the total number of recorded tornadoes. If also the average footprint size of tornadoes is known this can be used to deduct the hit rate R_F or the average occurrence interval AOI_F (i.e., the average return period, or the time when each location will be hit once on average). We discuss the three characteristics: tornado intensity distribution, footprint size, and AOI in the following subsections.

a. The intensity distribution of tornadoes

According to Groenemeijer and Kühne (2014)—for the period 1950 to 2013—the ESWD database contains records for 3818 tornadoes classified by their F scale. Only six of these tornadoes are classified as F5, making the estimated fraction of F5 tornadoes uncertain. Groenemeijer and Kühne (2014) furthermore point out that the number of low-intensity tornadoes in the database is likely unrepresentatively low, which leads to a biased intensity distribution. This is also supported by Grünwald and Brooks (2011). We therefore cannot deduct the tornado intensity distribution from these observations.

On the other hand—for the period 1950 to 2014—the U.S. Storm Prediction Center (SPC) database contains 59 945 tornadoes classified by intensity (http://www.spc.noaa.gov/wcm/). With nearly 16 times more data than the European dataset, this dataset can be used to obtain a statistically robust empirical tornado intensity distribution. We use bootstrapping to not only obtain the expected empirical intensity distribution but also its uncertainty. To do so, we sample 10 000 times 59 945 tornadoes (with replacement) from the dataset. However, this large dataset can also have an observational bias since weak tornadoes are likely to be underreported, especially in the early years covered by the dataset. To determine whether the tornado intensity distribution is stationary within this dataset we perform a bootstrapping experiment for four subsets covering different period lengths: 1950–2001, 1950–2014, 1985–2014, and 1995–2014. The period 1950–2001 is that used in Brooks (2004), and we use this as baseline for comparisons. Results are depicted in Fig. 1. They show that the tornado intensity distribution of registered tornadoes in the United States changed significantly over time (i.e., is nonstationary).

The temporal change of decadal tornado observations in the United States is investigated by Feuerstein et al. (2005). Based on previous work by Dotzek et al. (2003) the authors fit a stationary tornado intensity distribution together with a time- and intensity-dependent underreporting function to the observations. As a result they provide an unbiased tornado intensity distribution expressed by the Weibull density

Downloaded from http://journals.ametsoc.org/doi/pdf/10.1175/WCAS-D-15-0036.1 by guest on 22 October 2020

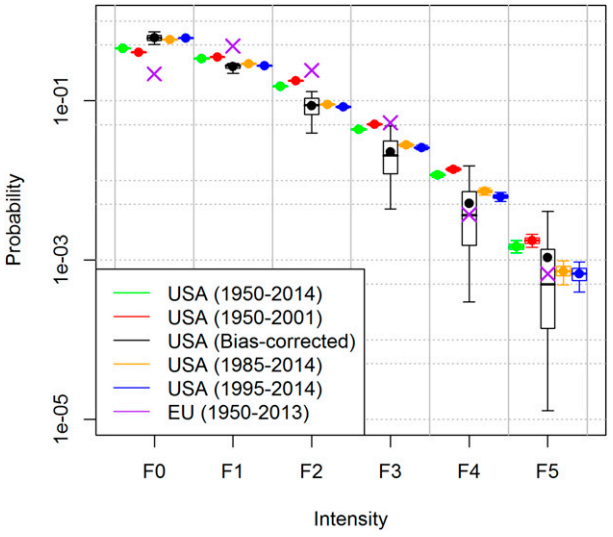

FIG. 1. Tornado intensity distribution. Purple crosses are best estimates based on the ESWD. The 5th, 25th, 50th, 75th, and 95th percentiles estimated by bootstrapping of the U.S. data. SPC values for various periods are drawn as colored box-and-whisker plots. Black box-and-whisker plots represent the bias-corrected tornado intensity distribution by Feuerstein et al. (2005). Black dots represent the expected value of the bias-corrected intensity distribution.

$$f(\mathrm{F}) = \frac{\beta}{\alpha}\left(\frac{\mathrm{F}+2}{\alpha}\right)^{\beta-1}\exp\left[-\left(\frac{\mathrm{F}+2}{\alpha}\right)^{\beta}\right], \qquad (5)$$

with scale and shape parameters of $\alpha = 2.13 \pm 0.20$ and $\beta = 1.79 \pm 0.12$, respectively. This density function is monotonically decreasing with increasing F for $\mathrm{F} > 0$. It is in good agreement with the Rayleigh distribution found by Kurgansky (2000) for the kinetic energy of tornadoes observed in Russia.

While the intensity distribution (5) is bias-corrected with respect to the time-dependent underreporting of weak tornadoes, its two parameters have a relatively high uncertainty. This becomes visible by drawing 100 000 realizations of $f(\mathrm{F})$ and integrating them over each F class to obtain the probability mass function over discrete F values. The results are shown in Fig. 1. In this paper, we use this limit distribution, including its uncertainty.

In passing, we note that, according to the continuous intensity distribution of Eq. (5), there is also a slight chance of 50 ppm for the occurrence of a tornado stronger than F5. Although there is no confirmed observation of an F6 tornado, radar-observed Doppler velocities of the F5 Bridge Creek tornado on 3 May 1999 in Oklahoma revealed wind speeds in the high F5 or low F6 range [for discussion, see Monastersky (1999), Davies-Jones et al. (2001), and Dotzek et al. (2003)].

TABLE 2. Percentiles and mean of the distribution of fraction of tornadoes of given intensity in percent after Feuerstein et al. (2005).

	F0	F1	F2	F3	F4	F5
5%	51.005	22.019	3.946	0.436	0.030	0.001
25%	56.775	25.731	6.710	1.205	0.153	0.014
50%	61.251	27.445	8.747	2.055	0.364	0.050
Mean	61.634	26.813	8.664	2.268	0.515	0.107
75%	66.107	28.496	10.690	3.112	0.723	0.137
95%	73.520	29.522	13.110	4.851	1.520	0.410

Here we attribute all modeled tornadoes stronger than F5 to the F5 class.

Some percentiles and the mean of the probability mass function of intensity over discrete F classes are provided in Table 2. The table indicates a median estimate of 88.9% of all tornadoes being weaker than F2 and 97.6% weaker than F3. Only 0.4% of tornadoes are stronger than F3; it is these few that are called "violent." Note that because of the low number of observed F5 tornadoes there is a factor of 410 between the 5th and the 95th percentiles of the estimates of the fraction of F5 tornadoes.

Based on the bias-corrected tornado intensity distribution, different regions only differ by the total number of tornadoes. This means—if we know the average number of tornadoes N_y that occur each year within a region of area A—that estimating the frequency of tornadoes of different intensity, n_{F}, is straightforward. The only necessary variable that has to be observed or estimated is N_y. This allows us to perform the following calculations based on a normalized tornado occurrence rate of one tornado per year per 10 000 km^2.

b. The size of tornadoes

We assume that tornado footprints have the shape of an ellipse characterized by a maximum width and length. Observations of footprint length and width are provided in both the ESWD and SPC database. The SPC provides average path widths before 1995 and maximum widths thereafter. Based on the assumption of an ellipse we transform average width to maximum width for all observations prior to 1995 by multiplying the observations by $4/\pi$.

Groenemeijer and Kühne (2014) provide averages of maximum width and length of European tornado footprints based on 698 observations of maximum width and 1088 observations of footprint length. These averages are shown in Fig. 2. For comparison, we also calculate averages and standard error of maximum width and length from the SPC database for the periods 1950–2014, 1950–2001, 1985–2014 and 1995–2014. Those are shown in Fig. 2, too.

Downloaded from http://journals.ametsoc.org/doi/pdf/10.1175/WCAS-D-15-0036.1 by guest on 22 October 2020

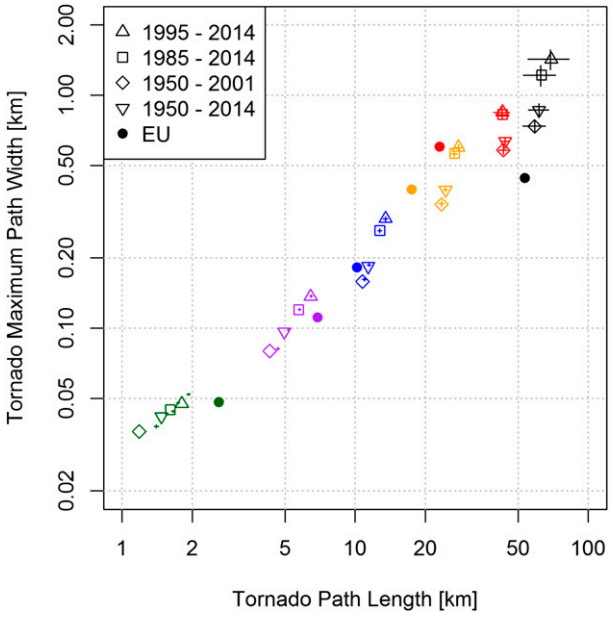

FIG. 2. Tornado footprints length and width for different F classes (F0: green, F1: purple, F2: blue, F3: yellow, F4: red, F5: black). Dots represent estimates for the ESWD database. Symbols represent expected values of Weibull fits to different periods of the U.S. SPC database, while crosses represent estimates of their empirical means and standard deviations.

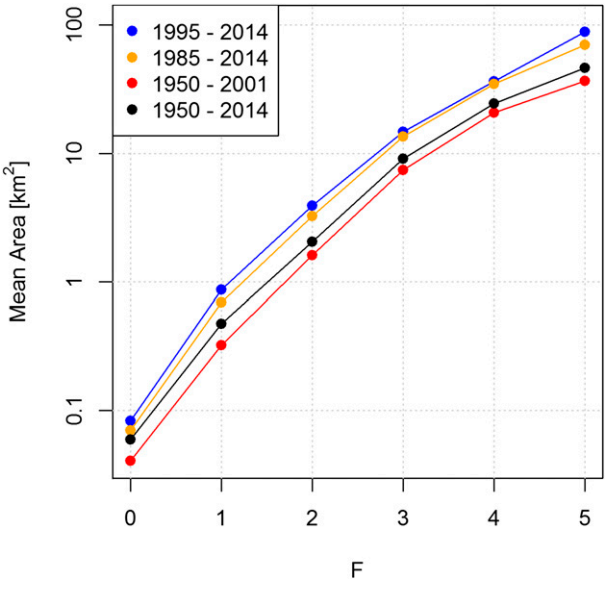

FIG. 3. Mean area of tornado footprints based on Weibull fits to length and width data of four different periods of the SPC database.

Brooks (2004) provides a distribution of the tornado footprint width w(F) and length l(F) as a function of the Fujita scale from observations in the United States from 1950 to 2001. Both parameters follow Weibull distributions with scale parameter α and shape parameter β. We employ the same fit for the four periods provided above. The expected values of width and length of the best-fit Weibull distributions are drawn in Fig. 2 as well. It can be seen that the expected values of the Weibull distributions are in line with the corresponding empirical averages except for F0 tornadoes, also already observed in Brooks (2004). As in Brooks (2004), quantile–quantile (QQ) plots generally show good agreement between empirical and Weibull distributions (not shown). Clear differences between the data from ESWD and SPC can be seen for path lengths of F0, F3, and F4 tornadoes and maximum path width of F5 tornadoes. A major result is that the path length and width of tornadoes in the SPC database both show significant positive trends.

Since there is no obvious argument to prefer the resulting size distribution corresponding to any of the four observation periods over the others, we carry the calculations forward with all four sets. This also allows investigating the impact of size uncertainty.

Given that length and width of a tornado footprint are modeled as Weibull-distributed random variables we can calculate the area distributions based on the assumption of elliptic footprints. One complication is that length and width of a tornado footprint are not independent. Instead they are correlated. This correlation can be estimated from the SPC observations. To get a reliable area distribution for each F class we create a two-dimensional normal-distributed correlated random variable and transform both marginal distributions to Weibull distributions with the shape and scale parameters estimated from the SPC observations for width and length. Those pairs are then used to calculate the area of the footprints. The distribution of the average footprint size per F class for the four periods considered is shown in Fig. 3. It shows that the difference between the period 1950–2001 used by Brooks (2004) and the 20 years from 1995 to 2014 is larger than a factor of 2 independent of tornado intensity.

c. *Hit rates* R_F *and AOI of tornadoes*

Observations of the rate of tornadoes for a given area can be misleading. The rate of rare strong events is noisy, especially for short records. The rate of weak events is usually underestimated due to underreporting. The latter has an upward trend due to increasing population, the spread of mobile phones and social media, increasing interest in tornadoes, and the general possibility to store and submit information via the Internet.

To estimate the rate R_F of tornado hits per location in a region, we follow the terminology of Grazulis (2001). The rate with which a location is hit by a tornado of intensity F depends on the ratio of the footprint size

Downloaded from http://journals.ametsoc.org/doi/pdf/10.1175/WCAS-D-15-0036.1 by guest on 22 October 2020

A_F of a tornado of this intensity and the area of the region, A_R, times the occurrence frequency n_F with which a tornado of this intensity occurs within this region:

$$R_F = \frac{1}{\mathrm{AOI}_F} = \frac{A_F}{A_R} n_F, \tag{6}$$

where n_F is the product of the number of tornadoes per year N_y times the intensity distribution $f(F)$. For the discussion in this section we use a standard area of $A_R = 10\,000\,\mathrm{km}^2$ and $N_y = 1$. In Eq. (6) the AOI is the reciprocal of the rate. AOI is of interest in itself, so that it is worthwhile to discuss it shortly: It represents the return period of a "hit" of an arbitrary point within the area with respect to a tornado of intensity F. In other words, it indicates the time when each location will be hit once on average. The reciprocal of the AOI_F is the local probability of a tornado hit of intensity F per year. This can be used to get the AOI_{tor} of a hit of a tornado of any intensity as

$$\mathrm{AOI}_{tor} = \frac{1}{1 - \prod_{F=0}^{5}\left(1 - \frac{1}{\mathrm{AOI}_F}\right)}. \tag{7}$$

This in turn can be used to provide an estimate of the probability that a subject at risk is hit by a tornado within its life span of N years as

$$p_{life} = 1 - \left(1 - \frac{1}{\mathrm{AOI}_{tor}}\right)^N \approx 1 - \exp\left(-\frac{N}{\mathrm{AOI}_{tor}}\right). \tag{8}$$

In section 3a we showed that the intensity distribution is uncertain and therefore a random variable. Thus, also R_F and AOI_F are random variables. Since they are inverse to each other it is obvious that for the expected value $\mu(\cdot)$ we get

$$\mu(R_F) = \mu\left(\frac{1}{\mathrm{AOI}_F}\right) \neq \frac{1}{\mu(\mathrm{AOI}_F)}. \tag{9}$$

In other words, the reciprocal of the expected rate does not equal the expected value of the AOI.

Quantiles and especially the median are not affected by this. Figure 4 shows box-and-whisker plots of rates and AOI calculated for the footprint area estimates of four different periods and the uncertain intensity distribution. While quantiles of AOI are the inverse of the quantiles of rates, the expected value of AOI lies in the tail of the distribution for F5 tornadoes. In this case the distribution of AOI is extremely skewed. With the median of the AOI about 50 times lower than its expected value, we can see that considering only the expected value of AOI can be very misleading.

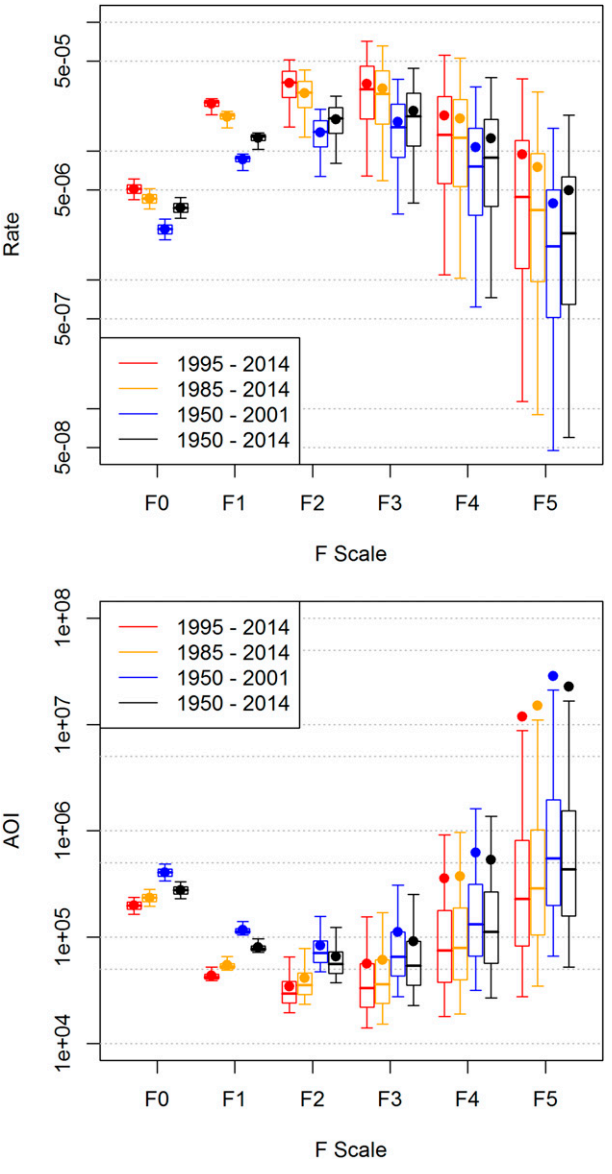

FIG. 4. Box-and-whisker plot of rates and AOI for the four different estimates of tornado footprint size, based on the bias-corrected tornado intensity distribution. Points indicate the expected value of the distribution; whiskers indicate the 5th and 95th percentiles. Boxes indicate the 25th, 50th, and 75th percentiles.

4. Vulnerability

a. *Vulnerability functions*

In natural catastrophe loss models, vulnerability functions translate hazard into loss ratios. They depend on the characteristics of the subjects at risk. Dotzek et al. (2003) provided vulnerability functions V_F for two classes of buildings in Europe: weak ones and strong ones. We use the one for strong buildings assuming that most of the insured buildings in Europe are built

Downloaded from http://journals.ametsoc.org/doi/pdf/10.1175/WCAS-D-15-0036.1 by guest on 22 October 2020

TABLE 3. Vulnerability (damage ratio) of strong buildings according to Dotzek et al. (2003) and effective vulnerability—taking into account the reduced vulnerability due to wind speed variations within a tornado footprint for two plausible forward speeds u_m, taken from the National Severe Storms Laboratory (NSSL) as described in the text.

		Effective vulnerability (%)	
Intensity	Vulnerability (%)	$u_m = 4.5\,\mathrm{m\,s^{-1}}$	$u_m = 9\,\mathrm{m\,s^{-1}}$
F0	0.035	0.035	0.035
F1	0.175	0.108	0.078
F2	1.9	0.682	0.417
F3	20	4.995	3.009
F4	70	14.137	9.418
F5	95	17.698	13.636

according to national building codes similar to the ones prescribed by Dotzek et al. (2003). Note that this vulnerability function only describes the structural damage to buildings and not the damage to the content and post-loss amplification (e.g., due to business interruption). Table 3 provides the values of Dotzek et al. (2003).

b. *Effective vulnerability functions for tornadoes*

The F scale classifies a tornado according to the wind speed that is attributed to the maximum damage it caused. However, wind speed varies within a tornado footprint and might be lower than the maximum wind speed for a considerable fraction of the footprint area. As a consequence, the resulting tornado damage is also not uniform across the tornado footprint.

To model this we assume that the tornado can be represented by a truncated Rankine vortex moving with a forward speed u_m. An estimate of the fraction of the footprint in which a maximum wind of certain F scale is reached is provided in the appendix.

Only a fraction of buildings hit by a tornado of certain intensity F actually gets hit with full strength. We can apply the F scale within a footprint to obtain the fraction of buildings a_F hit by lower wind speed (expressed as F class) than the one attributed to the tornado (F_t). This allows us to estimate an effective vulnerability:

$$V_{e,\mathrm{F}} = \sum_{\mathrm{F}=0}^{\mathrm{F}_t} V_\mathrm{F} a_\mathrm{F}. \tag{10}$$

In the above formulation, the vulnerability is no longer expressed uniquely with respect to a wind speed class but with respect to a "hit" of a tornado of intensity class F_t. Hence $V_{e,\mathrm{F}}$ is determined by the weighted average of the vulnerability function V_F within each given Fujita class. The weights are determined by the percentage of footprint area within each Fujita class. In this framework, we thus allow for the actual local maximum wind speed to be much lower for a large fraction of the footprint. Details are provided in the appendix. The resulting effective vulnerabilities are provided in Table 3 for two plausible forward speeds.

5. Results

a. *Relative loss ratios*

In this framework, we can calculate the relative contribution of each tornado intensity class to the overall tornado loss ratio as the product of the following variables only: the relative occurrence n_F, the footprint size A_F, and the effective vulnerability $V_{e,\mathrm{F}}$. No further information is needed. Using the effective vulnerabilities for two different plausible forward speeds leads to the results shown in Fig. 5, from which it becomes apparent that the different forward speeds have only a minor effect on the results.

Combining all datasets (100 000 realizations of the intensity distribution, to account for the uncertainty in the tornado dataset; four realizations of the area distribution, one for each of the four time periods defined to account for nonstationarity; and two effective vulnerabilities, to account for the sensitivity to tornado forward speeds) leads to the results provided in Table 4.

Taking the mean as the best estimate for the expected value, given the observations, then the comparison between Tables 2 and 4 reveals that about 60% of the tornadoes, the weakest and most frequent F0, cause only about 0.1% of the loss. About 88% of the tornadoes (F0 and F1) cause about 1% of the losses, while about 0.5% of the tornadoes (F4 and F5) cause about 60% of the loss. Despite the experience that hundreds of tornadoes are observed in Europe every year, significant tornado loss events have to be regarded and modeled as rare events.

Table 4 shows large uncertainties in the fraction of tornado losses from different F classes. As an example, the 95th percentile for F0 tornadoes is 45 times higher than the 5th percentile. Furthermore the 5th percentile for F1 tornadoes is considerably lower than the 95th percentile for F0 tornadoes. However, Table 4 does not provide information on the link among losses across different F classes. We therefore also look at the ratios of losses by adjacent F classes. Box-and-whisker plots of this ratio are shown in Fig. 6. According to this figure we can be virtually certain that losses increase with F class until F3 and that losses due to F5 tornadoes are lower than those due to F4. However, we have only about 75% confidence in the statement that losses due to F4 tornadoes are larger than those due to F3 tornadoes. The statement that F4 tornadoes contribute more than 40%

Downloaded from http://journals.ametsoc.org/doi/pdf/10.1175/WCAS-D-15-0036.1 by guest on 22 October 2020

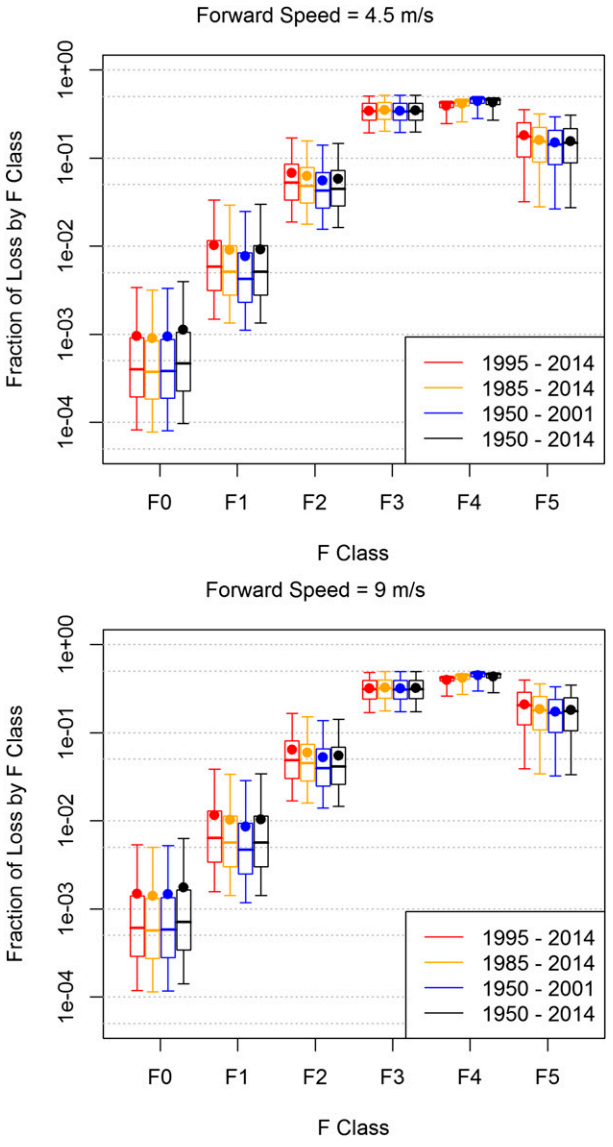

FIG. 5. Fraction of loss by F class for four different footprint size estimates and two different forward speeds.

of the total losses can also be made with 75% confidence. The median of losses due to F3 tornadoes is about 7 times higher than the median of F2 losses, which itself is about 9 times higher than the median of losses due to F1 tornadoes. It turns out that the latter is about 10 times higher than the median of losses due to F0 tornadoes.

b. *Economic loss to buildings in Europe*

The model discussed in sections 2 and 3 can be applied to any country for which an estimate of the total number of tornadoes per year, N_y, is available. In here we use estimates of N_y for several European countries from various sources. Estimates and sources are provided in Table 5 together with the country surface areas, A_C, and the resulting AOI and AALR. The tornado number density ρ_n, defined as the number of tornadoes per decade for a reference surface area of 10 000 km^2, can also be found in the same table. This normalized quantity can be taken as an indicator of tornado activity across Europe.

TABLE 4. Quantiles and mean of estimated contribution of tornadoes of given intensity to the overall building damage in percentage (%).

	F0	F1	F2	F3	F4	F5
5%	0.010	0.133	1.599	18.328	27.007	3.112
25%	0.024	0.283	2.851	25.658	40.188	9.880
50%	0.050	0.528	4.518	32.662	43.974	16.692
Mean	0.125	0.961	5.929	33.385	42.149	17.451
75%	0.115	1.061	7.412	40.871	46.818	24.157
95%	0.451	3.167	15.206	50.363	49.061	34.482

For most countries the tornado number density is between 5 and 10 per decade and 10 000 km^2. However, the estimate for Russia is much lower, which we attribute to underreporting. The tornado number density is much higher for the Netherlands, where most of the observed tornadoes are in fact waterspouts. To take into account the impact of these two outliers on the Europe-wide statistics, we also provide estimates excluding both countries, one at a time and together. Excluding both countries results in an estimated pan-European tornado number density ρ_n of 5.4 tornadoes per decade and 10 000 km^2.

According to Table 5 each location in Europe is hit by a tornado every 29 500 years on average. The estimated AALR of building damage is 2.11 ppm.

c. *Tornadoes in urban centers*

What is the probability of a violent tornado striking an urban center? The rate of hits for an urban center R_U can be estimated under the assumption that tornado strikes are equally likely everywhere within a country. In this case R_U follows directly from the number of tornadoes per year n_F in a country and the ratio of the area of an urban center A_U to the area of the country A_C as

$$R_U = n_F \frac{A_U}{A_C} = \frac{1}{\mathrm{AOI}_U} \tag{11}$$

and is the inverse of the average occurrence interval for an urban center AOI_U. Table 6 shows some of these average occurrence intervals for violent (F4 and F5) tornadoes.

Because the spatial distribution of thunderstorms is usually not homogeneous within European countries and waterspouts are happening only in the vicinity of the sea or large lakes the AOI_U provided in Table 6 should only be taken as an estimate of their order of magnitude.

Downloaded from http://journals.ametsoc.org/doi/pdf/10.1175/WCAS-D-15-0036.1 by guest on 22 October 2020

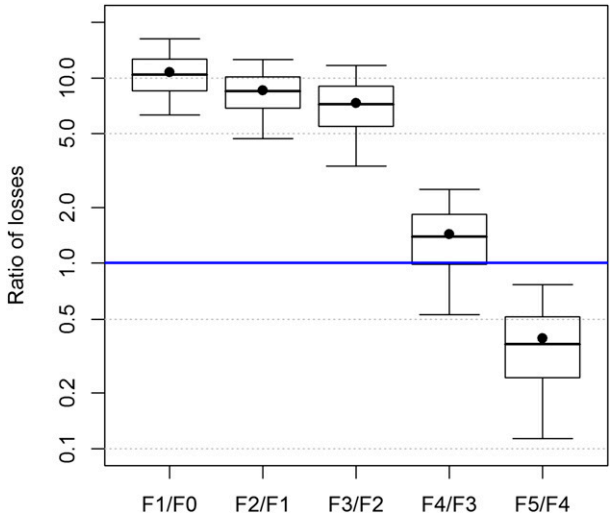

FIG. 6. Distribution of estimated ratio of losses due of neighboring F classes.

Estimated median AOI_U are on the order of 2000 to 15 000 years per urban center. Given the destructive power of violent tornadoes, we regard the threat of a violent tornado hitting an urban center in Europe as a rare but realistic scenario.

d. Probability of a hit of an individual building

Equations (7) and (8) can be used to estimate the return period of a tornado striking an individual building, as well as the probability of a hit during a certain period.

As an example, we estimate the probabilities that two among the oldest places of worship in Europe, London's St. Mary-le-Bow Church and Cologne Cathedral, had been hit by a violent tornado (F4 or F5) during their life span—from the year 1080 and 1248, respectively, until today. For Cologne Cathedral, the mean and median of this probability are 1.4% and 0.8%, respectively. For London's St. Mary-le-Bow Church these probabilities are 3.2% and 2.0%, respectively. While Cologne Cathedral has yet to see a tornado strike, a medieval version of St. Mary-le-Bow was destroyed by one of the earliest recorded, and one of the most violent, tornadoes in Britain, the so-called London Tornado of 1091 (see Table 1).

6. Discussion

We introduced a highly aggregated tornado loss model in order to estimate loss characteristics of tornadoes to buildings in Europe. In particular, we estimated return periods (average occurrence intervals) per country, city and location, as well as best estimates and uncertainties of average annual loss ratios. Given the sparsity of registered tornadoes in Europe we had to make several assumptions. Based on these assumptions the results need to be seen as ''best estimates'' of the order of magnitude, given the current knowledge. Here we are mostly interested in the relativities among the various tornado classes.

Long-term records of tornadoes in the United States and Europe reveal an increase in the number of registered tornadoes. However, according to Dotzek et al. (2003), Verbout et al. (2006), and Bissolli et al. (2007) this increase is only visible in the number of registered tornadoes of low intensity, while the number of strong tornadoes shows no significant increase.

Trenberth et al. (2007) found that the available studies are insufficient to detect possible trends in small-scale severe weather phenomena. Hartmann et al. (2013) see only low confidence for a positive trend in severe convective events. Both reports do not discuss tornadoes specifically but give reason to assume that the number of occurring tornadoes is constant.

We furthermore assume a universal (bias corrected) tornado intensity distribution. This assumption is supported by the analysis of tornado databases of various countries by Dotzek et al. (2003), Feuerstein et al. (2005), and Dotzek et al. (2005). We do not distinguish between different kinds of tornadoes (supercell tornadoes, nonsupercell tornadoes, waterspouts, gustnadoes), although they may lead to local deviations from the bias-corrected distribution used.

The third assumption is that the European tornado footprint characteristics (width and length) can be inferred from observations from the United States (Brooks 2004). The key variable is the average number of tornadoes per country, which we take from a survey by Dotzek (2003) and, where available, more recent available national sources. All results depend linearly on this variable, which allows for easy adaptation of the results in case new estimates become available.

Under the above assumptions, the resulting estimated return periods vary between different countries in Europe. Some extreme cases like the high AOI in Russia and the low one in the Netherlands might be explicable by underreporting and the inclusion of waterspouts, respectively. Generally there is a lower number of tornadoes registered in land-locked countries. Based on the information available, we did not try to correct for the fraction of waterspouts or gustnadoes in the individual national number of tornadoes per year. However, since the results depend linearly on the number of tornadoes per year per country, a correction can easily be made to account for the fraction of waterspouts in the national number of tornadoes, where this quantity is known.

Downloaded from http://journals.ametsoc.org/doi/pdf/10.1175/WCAS-D-15-0036.1 by guest on 22 October 2020

TABLE 5. National values of estimated number of occurring tornadoes by country per year N_y as taken from various sources; area A_C of European countries in km^2; tornado number density ρ_n in tornadoes per decade and 10 000 km^2; resulting mean and median AOI in 10^3 years, and resulting mean and median AALR in ppm. For comparison U.S. values are also shown. Sources of national annual tornado occurrences are 1) Dotzek (2003), 2) Holzer (2001), 3) Brázdil et al. (2012), 4) Rauhala et al. (2012), 5) Paul (2001), 6) Sioutas (2003), 7) TORRO (www.torro.org.uk), 8) Marcinoniene (2003), 9) G. Forbes (2010, personal communication), 10) Gayà (2011), 11) Kahraman and Markowski (2014), and 12) the NSSL.

					AOI		AALR	
Country	N_y	Source	A_C	ρ_n	Mean	Median	Mean	Median
Albania	2	1	28 748	7	22.78	18.72	2.73	1.81
Austria	2.7	2	83 871	3.2	49.23	40.47	1.27	0.84
Belgium	7.5	1	30 528	24.6	6.45	5.3	9.65	6.38
Bulgaria	2	1	110 879	1.8	87.87	72.22	0.71	0.47
Czech Republic	5.6	3	78 865	7.1	22.32	18.35	2.79	1.85
Estonia	9.5	1	45 227	21	7.55	6.2	8.25	5.46
Finland	14	4	338 424	4.1	38.31	31.49	1.63	1.08
France	17.5	5	551 695	3.2	49.96	41.07	1.25	0.82
Germany	30	1	357 114	8.4	18.87	15.51	3.3	2.18
Greece	14.5	6	131 999	11	14.43	11.86	4.32	2.85
Hungary	11.5	1	93 028	12.4	12.82	10.54	4.86	3.21
Ireland	10	7	70 273	14.2	11.14	9.15	5.59	3.7
Italy	15	1	301 336	5	31.84	26.17	1.96	1.29
Latvia	5	1	64 559	7.7	20.46	16.82	3.04	2.01
Lithuania	5	8	65 300	7.7	20.7	17.01	3.01	1.99
Netherlands (NL)	35	1	41 850	83.6	1.9	1.56	32.87	21.74
Poland	5.5	1	312 679	1.8	90.1	74.06	0.69	0.46
Portugal	4.3	9	92 090	4.7	33.94	27.9	1.83	1.21
Romania	3	1	238 391	1.3	125.94	103.52	0.49	0.33
Russia (European; RU)	12.5	1	3 960 000	0.3	502.09	412.69	0.12	0.08
Slovakia	4	1	49 037	8.2	19.43	15.97	3.21	2.12
Slovenia	1	1	20 273	4.9	32.13	26.41	1.94	1.28
Spain	30	10	505 992	5.9	26.73	21.97	2.33	1.54
Switzerland	3	1	41 284	7.3	21.81	17.93	2.86	1.89
Turkey	45	11	783 562	5.7	27.6	22.68	2.26	1.49
United Kingdom	40	7	242 900	16.5	9.62	7.91	6.47	4.28
Norway and Sweden	5	1	774 097	0.6	245.37	201.68	0.25	0.17
Denmark	2	1	43 094	4.6	34.15	28.07	1.82	1.21
Malta and Cyprus	2	1	9567	20.9	7.58	6.23	8.22	5.43
United States	1256	12	8 080 464	15.5	10.2	8.38	6.11	4.04
Europe (EU)	299.1		8 683 100	3.4	46.01	37.82	1.35	0.9
EU excluding RU	286.6		4 723 100	6.1	26.12	21.47	2.38	1.58
EU excluding NL	264.1		8 641 250	3.1	51.86	42.62	1.2	0.79
EU excluding RU and NL	251.5		4 681 250	5.4	29.5	24.25	2.11	1.4

City- and location-specific estimates are gained under the hypothesis that tornadoes are homogeneously distributed within each country. Since both the distribution of thunderstorms and waterspouts are not distributed homogeneously, results should be seen as an order-of-magnitude estimate. Detailed investigations, such as the one by Matsangouras et al. (2013), show a pronounced correlation between population density and the number of regionally observed tornadoes.

Returning to the questions posed in the introduction we conclude that it is possible to obtain risk estimates based on the available observations of tornadoes in Europe. While the uncertainty of the results depends only linearly on the total number of occurring tornadoes, model assumptions like the use of a Rankine vortex, the fixed tornado intensity distribution, and the use of one Europe-wide vulnerability function may have a significant impact.

Given these simplifications, the absolute values of the results presented in this publication have to be taken with care, and this research has to be seen as a first step toward a risk assessment of tornadoes in Europe. Better estimates of vulnerability functions of the European building stock will help improve future results.

However, the main finding of this study is that neither the strongest and rarest nor the weakest but most frequent tornadoes cause the most damage. While 90% of tornadoes cause together about 1% of the damage, about 3.6% of tornadoes, the F4, are the real loss

Downloaded from http://journals.ametsoc.org/doi/pdf/10.1175/WCAS-D-15-0036.1 by guest on 22 October 2020

TABLE 6. Estimated mean and median AOI in 10^3 years for hits of violent tornadoes (F4 and F5) for some urban centers in Europe.

City	Country	Area (km^2)	AOI (kyr)	
			Mean	Median
Munich	Germany	310	119	14.4
Hamburg	Germany	755	49	5.9
Berlin	Germany	892	41	5.0
London	United Kingdom	1738	14	1.7
Paris	France	2845	20	2.4
Rome	Italy	1285	24	2.9
Vienna	Austria	415	21	2.5

drivers with an expected 42% of loss contribution. According to our analysis, F0 to F2 tornadoes provide little contribution to the AALR, even if they constitute 97.6% of tornadoes. About 2% of the tornadoes are F3. They contribute about 30% of the losses. Because of their very rare occurrence it is virtually certain that F5 tornadoes contribute less to the total AALR than F4 tornadoes.

The real threat of tornadoes in Europe comes from the fact that devastating tornadoes are very rare, while short-term experience exists mainly for weak tornadoes. The very long return period of violent tornadoes in European countries feeds the misconception that tornadoes in Europe are weaker than in the United States although, according to Feuerstein et al. (2005), they are only less frequent.

Acknowledgments. The authors wish to thank RMS for the opportunity to work on this interesting subject. We also thank the four anonymous reviewers for their constructive comments and suggestions that led to an improved version of the article. Finally, special thanks go to Terence Baker for editing several drafts of this manuscript.

APPENDIX

Local Maximum Wind Speed in a Moving Rankine Vortex

We are interested in searching for the maximum wind speed $\hat{u}$ attained by a tornado for each location within its footprint, as ultimately it is this quantity that determines the maximum damage caused by a tornado and therefore its classification. For the sake of simplicity the wind speed $\mathbf{u}(\mathbf{r})$ for a stationary tornado is assumed to be a radial function of the distance r to the center. Furthermore, the tornado might move forward with translational speed $\mathbf{u}_m$. Its total wind speed at any location is therefore

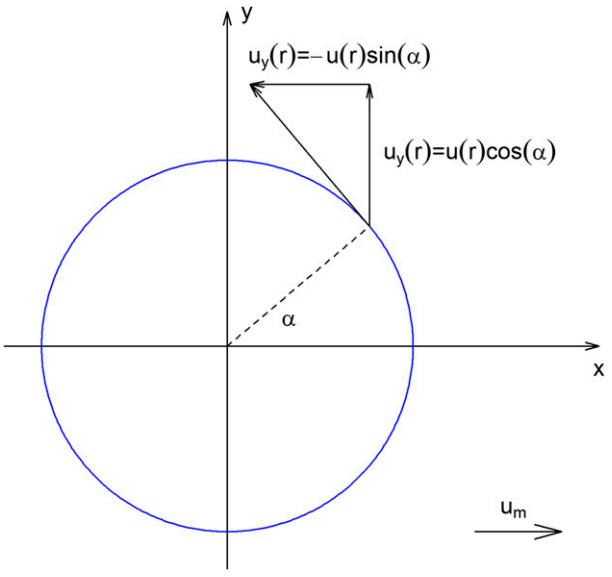

FIG. A1. Sketch of the coordinate system chosen for the estimation of maximum local wind speed.

$$\mathbf{u}_t = \mathbf{u}(r) + \mathbf{u}_m . \tag{A1}$$

If we choose a coordinate system rotated in the direction of movement, the velocity components are

$$\begin{aligned} u_x(r,\alpha) &= |\mathbf{u}_m| - |\mathbf{u}(r)|\sin(\alpha), \\ u_y(r,\alpha) &= |\mathbf{u}(r)|\cos(\alpha), \end{aligned} \tag{A2}$$

in which α is the angle measured counterclockwise from the moving direction (see Fig. A1).

Substituting (A2) in the expression of the absolute wind speed at any location

$$u(r,\alpha) = |\mathbf{u}_t| = \sqrt{u_x(r,\alpha)^2 + u_y(r,\alpha)^2} \tag{A3}$$

yields the expression

$$u(r,\alpha) = |\mathbf{u}_t| = \sqrt{u_m^2 - 2u_m u(r)\sin(\alpha) + u(r)^2}, \tag{A4}$$

where $u = |\mathbf{u}|$ is used for better readability.

Special cases are

$$\begin{aligned} u(r,\alpha = 0°) &= \sqrt{u_m^2 + u(r)^2}, \\ u(r,\alpha = 90°) &= u_m - u(r), \\ u(r,\alpha = 180°) &= \sqrt{u_m^2 + u(r)^2}, \quad \text{and} \\ u(r,\alpha = 270°) &= u_m + u(r). \end{aligned} \tag{A5}$$

To get a profile of maximum wind speed of a moving tornado we need to know the maximum wind speed

Downloaded from http://journals.ametsoc.org/doi/pdf/10.1175/WCAS-D-15-0036.1 by guest on 22 October 2020

along a line defined by the coordinate $y = y_0 = \text{constant}$. Therefore we need to build this constraint and solve for the maximum for all y. The constraint is easily formulated as

$$y = r\sin(\alpha) = \text{const}. \tag{A6}$$

Inserting this into Eq. (A4) yields

$$u(r, \alpha \,|\, y) = \sqrt{u_m^2 - 2u_m u(r)\frac{y}{r} + u(r)^2}, \tag{A7}$$

with $r \geq |y|$.

We now search for the maximum wind speed $\hat{u}(y) = \max[u(r, \alpha \,|\, y)]$ under the condition of constant y. This depends on the actual structure of $u(r)$. As in previous studies (e.g., Holland et al. 2006), here we assume a Rankine vortex, with a reference radius R of the form

$$u(r) = u_R \begin{cases} \dfrac{r}{R} & \text{if} \quad r \leq R \\ \dfrac{R}{r} & \text{if} \quad r > R \end{cases}. \tag{A8}$$

Inserting this expression into Eq. (A7), we obtain for the inner region ($r \leq R$)

$$u_i(r \,|\, y) = \sqrt{u_m^2 - 2u_m u_R \frac{y}{R} + u_R^2 \frac{r^2}{R^2}}. \tag{A9}$$

Obviously u_i is maximized if r takes its maximum value of $r = R$ and we get

$$\hat{u}_i(y) = \sqrt{u_m^2 - 2u_m u_R \frac{y}{R} + u_R^2} \quad \text{with} \quad -R \leq y \leq R. \tag{A10}$$

Now let us look for the outer region with $r > R$. By inserting $u_o = u_R(R/r)$ into Eq. (A7) we get

$$\begin{aligned} u_o[\sin(\alpha) \,|\, y] &= \sqrt{u_m^2 + \sin(\alpha)^2 \left(u_R^2 \frac{R^2}{y^2} - 2u_m u_R \frac{R}{y} \right)} \\ &= \sqrt{u_m^2 + \sin(\alpha)^2 A(y)}. \end{aligned} \tag{A11}$$

The sign of A determines for which angle α the maximum $\hat{u}(y) = \max\{u_o[\sin(\alpha) \,|\, y]\}$ is realized. Note that $\sin(\alpha)^2$ needs to be a maximum in order to maximize u_o in case of positive A. In case of negative A the maximum of u_o is realized for $\sin(\alpha)^2 = 0$ and thus $\alpha = 0°$ or 180°.

The value of A is always positive for $y < 0$. Therefore u_o is maximized for maximum $\sin(\alpha)^2$. In case of $y < -R$ this is realized by $\alpha = 270°$ (along the negative y axis), leading to

$$\hat{u}_o(y) = \sqrt{u_m^2 - 2u_m u_R \frac{R}{y} + u_R^2 \frac{R^2}{y^2}} \quad \text{with} \quad y < -R. \tag{A12}$$

For $0 > y > -R$ the y axis is within the inner region of the tornado and the maximum of $\sin(\alpha)^2$ is realized at $r = R$. It therefore falls together with the maximum of the inner region. This can be explicitly shown by inserting $\sin(\alpha) = y/R$ into Eq. (A11), which yields

$$\hat{u}_o(y) = \sqrt{u_m^2 - 2u_m u_R \frac{y}{R} + u_R^2} \quad \text{with} \quad -R \leq y \leq 0. \tag{A13}$$

In case of $0 < y < R$ we need to test whether A in Eq. (A7) is negative or positive. The value of A is positive if

$$\frac{y}{R} < \frac{1}{2}\frac{u_R}{u_m}. \tag{A14}$$

For $0 < y < R$ we see that y/R is always lower than 1. So we are on the safe side ($A > 0$) if $[(1/2)(u_R/u_m)] > 1$ (i.e., $u_R > 2u_m$). In other words, whenever the maximum rotational speed of the tornado is at least twice the forward moving speed, A is positive for $0 < y < R$, and we have to maximize $\sin(\alpha)$ in order to get

$$\hat{u}_o(y) = \sqrt{u_m^2 - 2u_m u_R \frac{y}{R} + u_R^2} \quad \text{with} \quad 0 \leq y \leq R. \tag{A15}$$

Thus in this case, $\hat{u}_o(y)$ has the same expression (A12) as $\hat{u}_i(y)$.

Finally we look into the case of $y > R$. For $y < [(u_R/u_m)(R/2)]$ we get a positive $A(y)$. Therefore u_o gets maximized by $\sin(\alpha) = 1$, leading to

$$\hat{u}_o(y) = \sqrt{u_m^2 - 2u_m u_R \frac{R}{y} + u_R^2 \frac{R^2}{y^2}} \quad \text{with} \quad R < y < \frac{u_R}{u_m}\frac{R}{2}. \tag{A16}$$

The value of $A(y)$ becomes negative for $y > [(u_R/u_m)(R/2)]$ and u_o is maximized if $\sin(\alpha) = 0$ (i.e., the wind speed decreases the closer the tornado gets). From Eq. (A11) we directly get

$$\hat{u}_o(y) = u_m \quad \text{with} \quad y > \frac{u_R}{u_m}\frac{R}{2}. \tag{A17}$$

In summary, the profile of maximum wind speed of a moving tornado, assuming a Rankine vortex profile, is given by

Downloaded from http://journals.ametsoc.org/doi/pdf/10.1175/WCAS-D-15-0036.1 by guest on 22 October 2020

TABLE A1. Area fraction a(F) of realized intensity F (in %) within a tornado footprint of a moving tornado with tornado intensity F and two plausible forward speeds u_m taken from NSSL as indicated in the text.

Intensity	u_m[m s^{-1}]	a(F0)	a(F1)	a(F2)	a(F3)	a(F4)	a(F5)
F0	4.5	100	0	0	0	0	0
	9	100	0	0	0	0	0
F1	4.5	47.86	52.14	0	0	0	0
	9	69.12	30.88	0	0	0	0
F2	4.5	47.91	18.81	33.28	0	0	0
	9	55.84	25.58	18.57	0	0	0
F3	4.5	47.99	18.72	9.47	23.83	0	0
	9	55.82	16.91	13.77	13.49	0	0
F4	4.5	47.90	18.66	9.5	5.71	18.24	0
	9	55.88	16.84	7.96	8.60	10.71	0
F5	4.5	47.88	18.76	9.48	5.72	3.70	14.46
	9	55.77	16.90	7.98	4.68	5.74	8.92

$$\hat{u}(y) = \begin{cases} \sqrt{u_m^2 - 2u_m u_R \dfrac{R}{y} + u_R^2 \dfrac{R^2}{y^2}} & \text{if} \quad y \le -R \\ \sqrt{u_m^2 - 2u_m u_R \dfrac{y}{R} + u_R^2} & \text{if} \quad -R < y \le R \\ \sqrt{u_m^2 - 2u_m u_R \dfrac{R}{y} + u_R^2 \dfrac{R^2}{y^2}} & \text{if} \quad R < y \le \dfrac{u_R}{u_m}\dfrac{R}{2} \\ u_m & \text{if} \quad y > \dfrac{u_R}{u_m}\dfrac{R}{2} \end{cases}. \tag{A18}$$

Note that $\hat{u}(y)$ can be used to attribute a maximum wind speed to each location within a tornado footprint. This allows for the estimation of the area fraction affected by maximum wind speeds within the range of each F class as a function of the forward speed u_m. Results for two representative forward speeds u_m (taken from the NSSL at http://www.nssl.noaa.gov/education/svrwx101/tornadoes/faq/) are provided in Table A1 as function of the F scale. The parameter R follows from the width of the tornado determined at the outer points at which wind speeds reach F0.

REFERENCES

Bissolli, P., J. Grieser, N. Dotzek, and M. Welsch, 2007: Tornadoes in Germany 1950–2003 and their relation to particular weather conditions. *Global Planet. Change*, **57**, 124–138, doi:10.1016/j.gloplacha.2006.11.007.

Brázdil, R., K. Chromá, P. Dobrovolnỳ, and Z. Černoch, 2012: The tornado history of the Czech lands, AD 1119–2010. *Atmos. Res.*, **118**, 193–204, doi:10.1016/j.atmosres.2012.06.019.

Brooks, H. E., 2004: On the relationship of tornado path length and width to intensity. *Wea. Forecasting*, **19**, 310–319, doi:10.1175/1520-0434(2004)019<0310:OTROTP>2.0.CO;2.

Davies-Jones, R., R. Trapp, and H. Bluestein, 2001: Tornadoes and tornadic storms. *Severe Convective Storms*, *Meteor. Monogr.*, No. 50, Amer. Meteor. Soc., 167–221.

Doswell, C. A., III, H. E. Brooks, and N. Dotzek, 2009: On the implementation of the enhanced Fujita scale in the USA. *Atmos. Res.*, **93**, 554–563, doi:10.1016/j.atmosres.2008.11.003.

Dotzek, N., 2003: An updated estimate of tornado occurrence in Europe. *Atmos. Res.*, **67-68**, 153–161, doi:10.1016/S0169-8095(03)00049-8.

——, J. Grieser, and H. E. Brooks, 2003: Statistical modeling of tornado intensity distributions. *Atmos. Res.*, **67-68**, 163–187, doi:10.1016/S0169-8095(03)00050-4.

——, M. V. Kurgansky, J. Grieser, B. Feuerstein, and P. Névir, 2005: Observational evidence for exponential tornado intensity distributions over specific kinetic energy. *Geophys. Res. Lett.*, **32**, L24813, doi:10.1029/2005GL024583.

ESSL, 2015: Corporate report on the 8 July 2015 tornado of Mira (VE), Italy. European Severe Storms Laboratory, 7 pp. [Available online at http://www.essl.org/cms/wp-content/uploads/20150902-Mira-Tornado-of-8-July-2015-Report.pdf.]

Feuerstein, B., N. Dotzek, and J. Grieser, 2005: Assessing a tornado climatology from global tornado intensity distributions. *J. Climate*, **18**, 585–596, doi:10.1175/JCLI-3285.1.

Fujita, T. T., and A. D. Pearson, 1973: Results of FPP classification of 1971 and 1972 tornadoes. Preprints, *Eighth Conf. on Severe Local Storms*, Denver, CO, Amer. Meteor. Soc., 142–145.

Gayà, M., 2011: Tornadoes and severe storms in Spain. *Atmos. Res.*, **100**, 334–343, doi:10.1016/j.atmosres.2010.10.019.

Grazulis, T., 2001: *The Tornado, Nature's Ultimate Windstorm.* University of Oklahoma Press, 324 pp.

Groenemeijer, P., and T. Kühne, 2014: A climatology of tornadoes in Europe: Results from the European Severe Weather Database. *Mon. Wea. Rev.*, **142**, 4775–4790, doi:10.1175/MWR-D-14-00107.1.

Grünwald, S., and H. E. Brooks, 2011: Relationship between sounding derived parameters and the strength of tornadoes in Europe and the USA from reanalysis data. *Atmos. Res.*, **100**, 479–488, doi:10.1016/j.atmosres.2010.11.011.

Hartmann, D., and Coauthors, 2013: Observations: Atmosphere and surface. *Climate Change 2013: The Physical Science Basis*, T. Stocker et al., Eds., Cambridge University Press, 159–254.

Holland, A. P., A. J. Riordan, and E. C. Franklin, 2006: A simple model for simulating tornado damage in forests. *J. Appl. Meteor. Climatol.*, **45**, 1597–1611, doi:10.1175/JAM2413.1.

Holzer, A. M., 2001: Tornado climatology of Austria. *Atmos. Res.*, **56**, 203–211, doi:10.1016/S0169-8095(00)00073-9.

Kahraman, A., and P. M. Markowski, 2014: Tornado climatology of Turkey. *Mon. Wea. Rev.*, **142**, 2345–2352, doi:10.1175/MWR-D-13-00364.1.

Kurgansky, M., 2000: The statistical distribution of intense moist convective, spiral vortices in the atmosphere. *Dokl. Earth Sci.*, **371**, 408–410.

Marcinoniene, I., 2003: Tornadoes in Lithuania in the period of 1950–2002 including analysis of the strongest tornado of 29 May 1981. *Atmos. Res.*, **67-68**, 475–484, doi:10.1016/S0169-8095(03)00060-7.

Matsangouras, I. T., P. T. Nastos, H. B. Bluestein, and M. V. Sioutas, 2013: A climatology of tornadic activity over Greece based on historical records. *Int. J. Climatol.*, **34**, 2538–2555, doi:10.1002/joc.3857.

McDonald, J. R., K. C. Metha, and S. Mani, 2006: A recommendation for an enhanced Fujita scale (EF-scale), revision 2. Texas Tech University Wind Science and Engineering Research Center Rep., 111 pp. [Available online at http://www.depts.ttu.edu/nwi/Pubs/FScale/EFScale.pdf.]

Downloaded from http://journals.ametsoc.org/doi/pdf/10.1175/WCAS-D-15-0036.1 by guest on 22 October 2020

Meaden, G. T., 1976: Tornadoes in Britain: Their intensities and distribution in space and time. *J. Meteor.*, **1**, 242–251.

Monastersky, R., 1999: Oklahoma tornado sets wind record. *Sci. News*, **155**, 308, doi:10.2307/4011396.

Paul, F., 2001: A developing inventory of tornadoes in France. *Atmos. Res.*, **56**, 269–280, doi:10.1016/S0169-8095(00)00077-6.

Rauhala, J., H. E. Brooks, and D. M. Schultz, 2012: Tornado climatology of Finland. *Mon. Wea. Rev.*, **140**, 1446–1456, doi:10.1175/MWR-D-11-00196.1.

Sioutas, M. V., 2003: Tornadoes and waterspouts in Greece. *Atmos. Res.*, **67-68**, 645–656, doi:10.1016/S0169-8095(03)00078-4.

Trenberth, K., and Coauthors, 2007: Observations: Surface and atmospheric climate change. *Climate Change 2007: The Physical Science Basis*, S. Solomon et al., Eds., Cambridge University Press, 235–336.

Verbout, S. M., H. Brooks, L. M. Leslie, and D. M. Schultz, 2006: Evolution of the U.S. tornado database: 1954–2003. *Wea. Forecasting*, **21**, 86–93, doi:10.1175/WAF910.1.

Downloaded from http://journals.ametsoc.org/doi/pdf/10.1175/WCAS-D-15-0036.1 by guest on 22 October 2020